Important Role of Fe(III)TPP–Oxygen–Skatole Ternary Complex in Tryptophan Dioxygenase Model Reaction System

KUNIHIKO TAJIMA*, MIWA YOSHINO, KOHICHI MIKAMI, TAKESHI EDO, KAZUHIKO ISHIZU
Department of Chemistry, Faculty of Science, Ehime University, Matsuyama 790 (Japan)
and HIROAKI OHYA-NISHIGUCHI
Department of Chemistry, Faculty of Science, Kyoto University, Sakyo-ku Kyoto 606 (Japan)
(Received August 11, 1989; revised December 4, 1989)

Abstract

The mechanism of the dioxygenation of 3-methylindole occurring in the presence of Fe(III)TPPCl and alkaline reagents was studied by means of product analyses and spectroscopic measurements. The results of GC-MS measurements indicated that 3-methylindole (skatole) was converted to *o*-formamidoacetophenone (FA), in which two oxygen atoms derived from atmospheric oxygen were involved. The optical spectrum recorded for the mixture at −78 °C demonstrated the presence of a new iron complex as characterized by absorption maxima at 421, 550 and 586 nm. The ESR spectrum recorded for the same reaction mixture revealed the formation of two types of ferric low-spin complexes ($g_1 = 2.32$, $g_2 = 2.17$, $g_3 = 1.95$; $g_1 = 2.24$, $g_2 = 2.16$, $g_3 = 1.96$) with anomalously small g anisotropy. From comparison of ESR parameters of the complexes with those of previously reported heme–butyl peroxide complexes, the present complexes were assumed to be the six-coordinate Fe(III)TPP–peroxide complex. Based on superhyperfine splittings (27 gauss) derived from $^{17}O_2$ enriched oxygen ($^{17}O_2$, $I = 5/2$), these complexes were concluded to be the Fe(III)TPP($^-OCH_3$)-($^-$OO-skatole) and Fe(III)TPP($^-$OO-skatole)$_2$ complexes, having 3-methyl-3-hydroperoxo-indolenine at the axial position. The Fe(III)TPP–oxygen–substrate ternary complex will be an important intermediate species generated in the dioxygenation processes of skatole.

Introduction

Tryptophan dioxygenase, TDO [1] has been well established as a unique dioxygenase having a prosthetic heme group in the reaction site. TDO catalyzes the metabolism of tryptophan into the corresponding *o*-formamidoacetophenone (FA) utilizing molecular oxygen. A possible reaction mechanism of TDO was tentatively expressed as follows (Scheme 1) [2]. The resting form of TDO (denoted as EM), having a ferrous heme group at the reaction site, was changed to the EM–substrate (EMS) complex when the substrate (S) molecule bound at the reaction site. Then the EMS complex captured molecular oxygen at the axial position of heme ($EMSO_2$). The axially ligating molecular oxygen was thought to be activated and was inserted into the substrate molecule through the transient intermediate $EMSO_2^*$ complex formation. After liberation of the dioxygenated product (P) from the reaction site, TDO again changed into its resting form (EM). In the reaction cycles of TDO, the electronic and coordination structures of both the $EMSO_2$ and $EMSO_2^*$ complexes have attracted intense interest of many workers. The formation of the former $EMSO_2$ complex [2] was demonstrated by means of optical absorption measurements, however the latter transient $EMSO_2^*$ complex has not been detected by spectroscopic procedures. The $EMSO_2^*$ complex was regarded as the most important intermediate in the dioxygenation processes of TDO. So far, many trials have been made to understand the reaction profile of TDO by using synthetic transition metal complexes such as Co(II)salen [3], Mn(II)PC

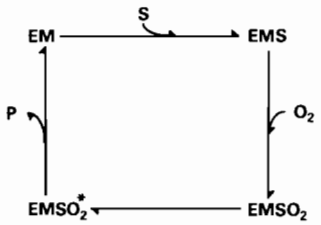

Scheme 1. Schematic expression of the reaction cycle assumed for tryptophan dioxygenase (TDO). Abbreviations: EM, resting form of TDO; S, substrate tryptophan molecule; O_2, atmospheric molecular oxygen; $EMSO_2$, oxygenated form of substrate binding EMS; $EMSO_2^*$, activated ternary type intermediate species; P, dioxygenated products of the tryptophan.

*Author to whom correspondence should be addressed.

0020-1693/90/$3.50

[4], Co(II)TPP [5] and Fe(II)TPP(pyridine)$_2$ [6] complexes, but a practical model of the $EMSO_2$* complex has not been reported.

Here, mechanistic studies on the dioxygenation process of TDO were carried out for a model reaction system composed of Fe(III)TPPCl, tetramethyl ammonium hydroxide (TMAOH) and 3-methylindole (skatole). In our model system, 3-methylindole (skatole) was efficiently converted to *o*-formamidoacetophenone (FA), which has two oxygen atoms derived from atmospheric oxygen. The simultaneous optical absorption and ESR measurements demonstrated that two types of intermediate complexes were generated in the present TDO model reaction system. The observed ESR and optical property of the complexes were analogous to those of Fe(III)-TPP–butylperoxide complexes. From comparison of ESR and optical parameters of the complexes with related heme–peroxide complexes [7, 8], the intermediate complexes were assumed to be a heme–oxygen–substrate ternary complex, which can be a noble model complex of the $EMSO_2$* intermediate complex assumed for TDO. The role of the ternary complex in the dioxygenation processes of skatole will be discussed on the basis of the results obtained from ESR and optical measurements and product analysis.

Experimental

Measurements

Optical absorption spectra at −78 °C were recorded using an Ohtsuka Electronic Co. Ltd., MCPD-100 spectrophotometer, with wavelength range from 400 to 800 nm. ESR spectra were measured at 77 K using a JEOL FE2XG X-band spectrometer operating with 100 kHz field modulation. The microwave frequency applied to the sample (5.0 mW) was monitored by an Advantest TR-5212 digital frequency counter. The magnetic field strength was calibrated by the hyperfine coupling constant (86.9 gauss) of the Mn(II) ion doped in MgO powder. The g values of the observed ESR spectra were estimated based on the g value of Li-TCNQ radical salt (g = 2.0025) as a standard. All the measurements were performed at Advantest Instrumental Center for Chemical Analysis, Ehime University.

Materials

Fe(III)TPPH$_2$ and its iron complex, Fe(III)TPPCl, were prepared and purified in our laboratory by the ordinary procedures described by Adler *et al.* [9]. The purity of Fe(III)TPPCl was checked by means of ^{1}H NMR and elements analysis. 3-Methylindole was obtained from Tokyo Kasei Co. Ltd., and supplied for measurements after recrystallization. A methanol solution of tetramethylammonium hydroxide (TMAOH) was purchased at Wako Pure Chemicals and used after calibration of alkaline concentration by pH titration method. Isotopes of oxygen $^{18}O_2$ (96.0%) and $^{17}O_2$ (49%) were used for the oxygenation reaction. The authentic samples of *o*-formamidoacetophenone were prepared by the procedures described by Nishinaga [3]; *o*-aminoacetophenone was obtained from Merck Co. Ltd. Other chemicals used for the measurements and reactions were guaranteed grade.

Results and Discussion

Product Analysis for the TDO Model Reaction System

In a 10 mm diameter glass tube equipped with an oxygen balloon, a dichloromethane solution of skatole (0.2 M, 0.4 ml), Fe(III)TPPCl (0.2 mM, 0.8 ml) and a methanol solution of TMAOH (0.2 M, 0.04 ml) were mixed and stirred at 25 °C. The concentration of skatole involved in the reaction mixture was monitored by means of GLC measurements. Figure 1(a) shows the concomitant increase in the skatole conversion ($100 \times C_i/C_0$), in which C_i and C_0 means the concentration of skatole estimated at after i min, and the initial concentration skatole, respectively. After about 80 min, the skatole conversion reached about 35% (Fig. 1(a)) in this case,

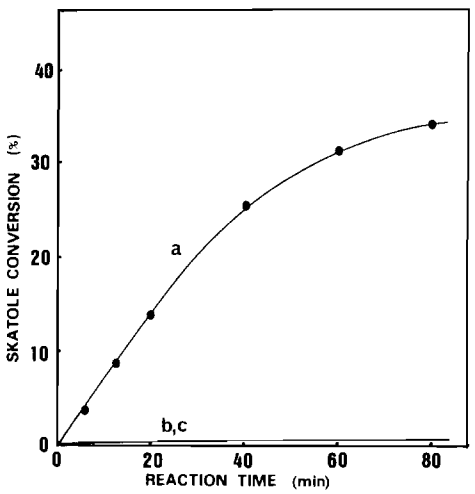

Fig. 1. Relationship between the reaction time and skatole conversion ($100 \times C_i/C_0$), in which C_i means the concentration of skatole at i min, and C_0 means the initial concentration of skatole: (a) observed for reaction mixture, composed of Fe(III)TPPCl (0.2 mM, 0.8 ml), TMAOH (0.2 M, 0.04 ml) and skatole (0.2 M, 0.4 ml), stirred under oxygen atmosphere at 25 °C. The mixing molar ratio of chemicals Fe(III)TPPCl: TMAOH:skatole = 1:5:50, and the solvent composition is dichloromethane:methanol = 1200:40; (b) observed in the absence of Fe(III)TPPCl; (c) observed in the absence of TMAOH.

but a detectable amount of skatole conversion was never observed in the absence of Fe(III)TPP (Fig. 1(b)) or TMAOH (Fig. 1(c)). The time dependent GLC measurements provide the experimental support that the presence of Fe(III)TPPCl and TMAOH was indispensable for the skatole conversion to proceed in our model reaction system.

The major product derived from skatole was isolated from the reaction mixture and was assigned to be *o*-formamidoacetophenone (FA) based on the results of ^{1}H NMR and elemental analysis. In addition, one of the minor products generated in the reaction system was also assigned to be *o*-aminoacetophenone (AA). The yield of FA in relation to consumed skatole was estimated to be 95% (0.26×10^{-3} mol), which corresponds to about 70 times as large as the initial concentration of Fe(III)TPPCl. The results of product analysis demonstrate that Fe(III)-TPPCl catalyzes the conversion of skatole to FA in the presence of TMAOH under oxygen atmosphere.

In order to assign the source of oxygen involved in FA, GC-MS* measurements were carried out for FA generated under $^{18}O_2$ (96% enriched) oxygen atmosphere. As shown in Fig. 2(a), FA produced under $^{16}O_2$ conditions gave a mother ion peak at $M = 163$, and three major fragment peaks appeared at 148, 135 and 120. On the other hand, the mother ion peak due to the FA prepared under $^{18}O_2$ atmosphere appeared at $M = 167$ (Fig. 2(b)), which agrees with that calculated for $C_9H_9N(^{18}O)_2$, $MW = 167$. Furthermore, the three major fragment peaks, containing one or two oxygen atoms, also shifted to 152, 137 and 122, respectively. From comparison of the observed GC-MS spectra of FA prepared under $^{16}O_2$ with those under $^{18}O_2$ atmosphere (Fig. 2(a) and (b)), it is obvious that two oxygen atoms derived from $^{18}O_2$ were introduced into the FA molecule. Based on the results of GC-MS measurements, oxygen atoms involved in methanol and TMAOH can be ruled out as being the candidates of the oxygen source of FA. Therefore, one can conclude that Fe(III)TPPCl catalyzes the dioxygenation of 3-methylindole (skatole) utilizing molecular oxygen in the presence of an alkaline reagent, as is schematically expressed in Scheme 2.

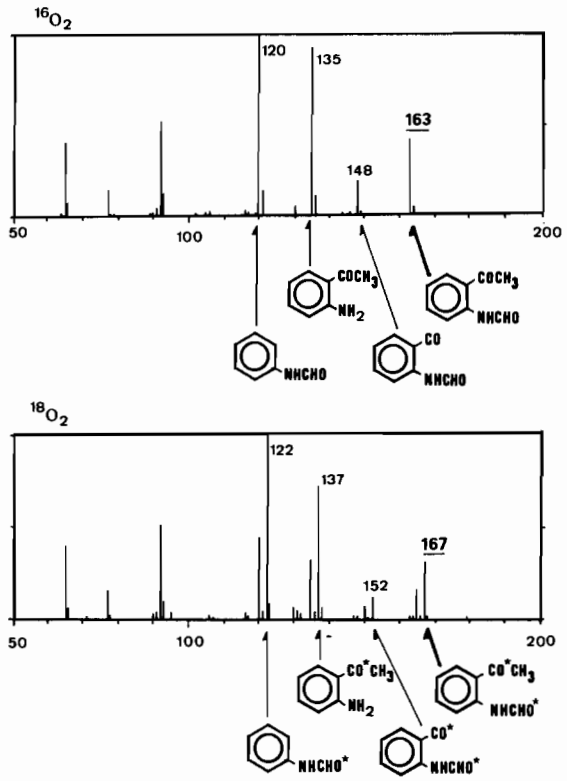

Fig. 2. GC-MS fragment patterns observed for *o*-formamidoacetophenone (FA) generated in the present reaction system consisting of Fe(II)TPPCl, TMAOH and skatole: (a) GC-MS spectrum observed for FA prepared under $^{16}O_2$ atmosphere; (b) GC-MS spectrum recorded for FA prepared under $^{18}O_2$ (96% enriched). The asterisks marked on the oxygen atom means the ^{18}O isotope derived from atmospheric $^{18}O_2$.

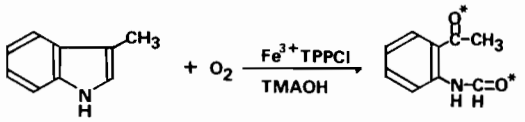

Scheme 2. The formulated overall reaction profile of the present TDO model skatole dioxygenation system consisting of Fe(III)TPPCl, skatole and TMAOH, which occurred when utilizing atmospheric molecular oxygen. Oxygen atoms with asterisk are derived from atmospheric molecular oxygen.

*Abbreviations; Fe(III)TPPCl, chloro(5,10,15,20-tetraphenyl)porphyrinato iron(III); ESR, electron spin resonance; GLC, gas chromatograph; GC-MS, gas chromatograph-mass spectroscopy; FA, *o*-formamidoacetophenone; AA, *o*-aminoacetophenone; skatole, 3-methylindole; $^-$OO-skatole, the deprotonated form of 3-methyl-3-hydroperoxo-indolenine; $^-$OO-tert-butyl, deprotonated form of tert-butylhydroperoxide; TMAOH, tetramethylammonium hydroxide; TBAOH, tetrabutylammonium hydroxide.

Detection of Intermediate Complex by Means of ESR and Optical Measurements

ESR and optical measurements were carried out to understand the dioxygenation processes of skatole occurring in the reaction system. As a reference, ESR and optical spectra were recorded under nitrogen atmosphere for the cooled solution (−78 °C) of Fe(III)TPPCl (0.5 mM, 0.4 ml). The Soret-band and Q-band absorption maxima were clearly detected at 417, 510, 580 and 690 nm, as shown in Fig. 3(a). The observed absorption maxima and lineshape agreed well with that of Fe(III)TPPCl recorded at 25 °C (see

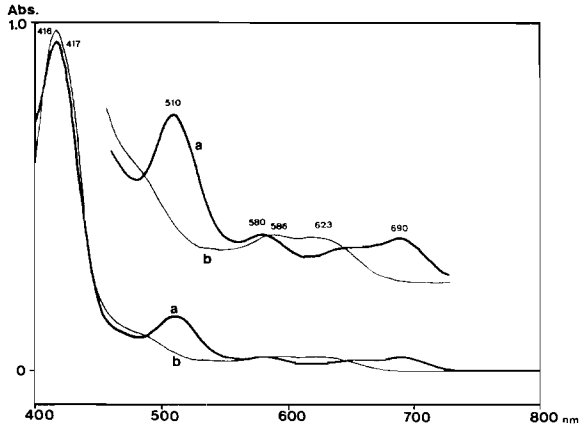

Fig. 3. Optical absorption spectra recorded at −78 °C: (a) spectrum recorded for dichloromethane solution of Fe(III)-TPPCl (0.5 mM, 0.4 ml); (b) spectrum recorded after addition of TMAOH (0.1 M, 0.02 ml).

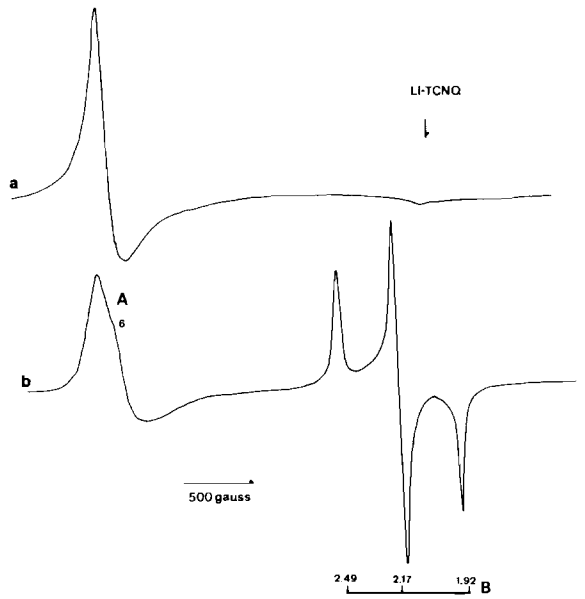

Fig. 4. ESR spectra recorded for frozen mixture of Fe(III)-TPPCl, TMAOH and skatole at 77 K: (a) spectrum recorded for Fe(III)TPPCl (0.5 mM, 0.4 ml); (b) spectrum recorded after addition of TMAOH (0.1 M, 0.02 ml).

Table 2). The ESR spectrum observed for the reaction mixture at 77 K showed the characteristic ESR lineshape ascribed to the ferric high-spin complex ($g_\perp = 6$ and $g_\parallel = 2$), as shown in Fig. 4(a). By addition of TMAOH (0.1 M, 0.02 ml), the Soret- and Q-band were shifted to 416, 586 and 623 nm (Fig. 3(b)). The ESR spectrum recorded for the same solution at 77 K revealed the presence of the ferric high-spin complex (**A**; $g_\perp = 6$, $g_\parallel = 2$) and ferric low-spin complex (**B**; $g_1 = 2.487$, $g_2 = 2.167$, $g_3 = 1.915$), as shown in Fig. 4(b). Based on the observed g parameters of the low-spin complex, complex **B** was assigned to be Fe(III)TPP($^-OCH_3$)$_2$, having the methoxide anion at both axial positions of the heme [8, 10]. On the other hand, complex **A** was also assigned to be the six-coordinate Fe(III)TPP($^-OCH_3$)-($HOCH_3$) [8, 10].

A dichloromethane solution of skatole (2.0 M, 0.04 ml) was added to the reaction mixture under nitrogen atmosphere at −78 °C. Then dry oxygen gas (about 20 ml) was slowly introduced into the reaction mixture through a fine capillary. After about 1 min induction period, the color of the reaction solution gradually turned to bright red as seen for the case of oxyhemoglobin. The optical absorption spectrum observed after 3 min at −78 °C (Fig. 5(a)) showed Soret- and Q-band absorption maxima at 421, 550 and 586 nm. The reaction mixture was rapidly frozen in liquid nitrogen and the ESR spectrum was recorded at 77 K. As shown in Fig. 6(a), the ESR signal due to the ferric low-spin complexes (**C**: $g_1 = 2.316$, $g_2 = 2.169$, $g_3 = 1.952$; and **D**: $g_1 = 2.238$, $g_2 = 2.160$, $g_3 = 1.964$) were clearly recorded, with a small amount of complex A remaining. The optical spectrum recorded after 6 min (Fig. 5(b)) almost agreed with that recorded after 3 min (Fig. 5(a)). On the contrary, the ESR spectrum observed after 6 min (Fig. 6(b)) was different from that recorded after 3 min (Fig. 6(a)). The ESR signal intensity of complex **D** reached a maximum, while that of complex **C** almost disappeared (Fig. 6(b)). From comparison of the ESR signal intensity of complex **D** recorded after 3 min with that of 6 min (Fig. 6(a) and (b)), we found that the ESR signal intensity of complex **D** showed concomitant increase when keeping the reaction mixture at −78 °C under

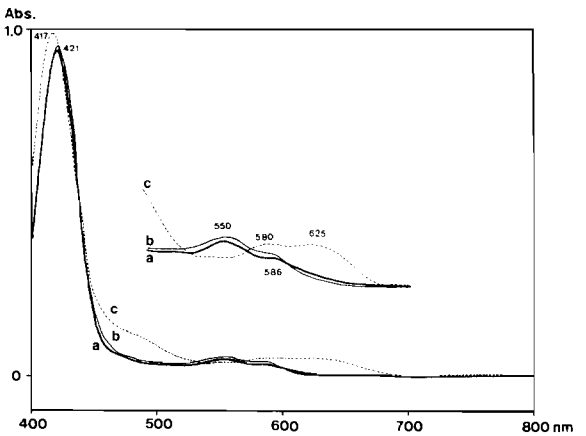

Fig. 5. Optical spectra observed at −78 °C after contact between the reaction mixture and dry oxygen at −78 °C: (a) spectrum recorded after 3 min for the reaction mixture composed of Fe(III)TPPCl (0.5 mM, 0.4 ml), TMAOH (0.1 M, 0.02 ml) and skatole (2.0 M, 0.04 ml); (b) spectrum recorded after standing the mixture at −78 °C for 6 min; (c) spectrum recorded after the reaction mixture of (b) was thawed at 25 °C for about 5 min.

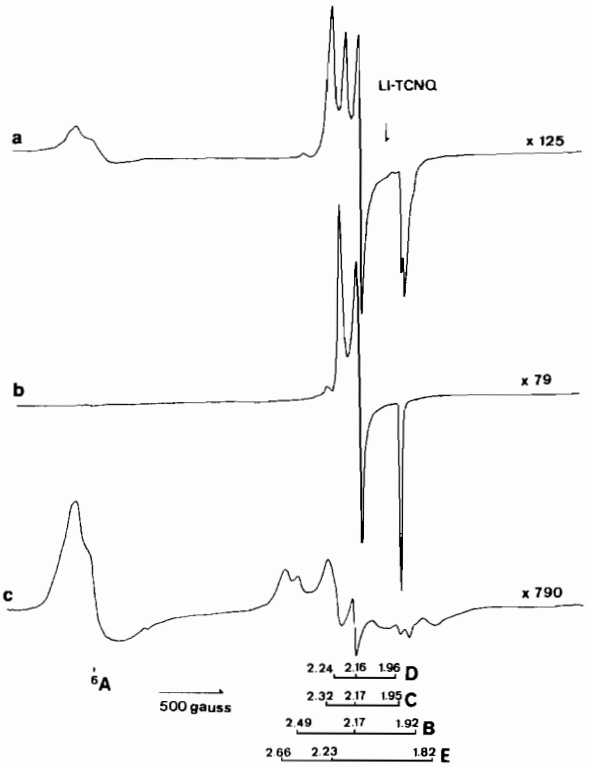

Fig. 6. ESR spectra recorded at 77 K after contact between the reaction mixture and dry oxygen gas at −78 °C: (a) spectrum recorded after 3 min for the reaction mixture containing Fe(III)TPPCl (0.5 mM, 0.4 ml), TMAOH (0.1 M, 0.02 ml) and skatole (2.0 M, 0.04 ml); (b) spectrum recorded after 6 min; (c) spectrum recorded after the reaction mixture of (b) was thawed at 25 °C for about 5 min. The amplitude of the ESR measurements was varied as written on the right hand side of each ESR spectrum.

oxygen atmosphere. It is noted here that complexes **C** and **D** were clearly resolved in the ESR spectra recorded at 77 K, but optical spectral measurements at −78 °C failed to distinguish complexes **C** and **D**. Accordingly, the optical spectra observed at −78 °C (Fig. 6(a)) are tentatively explained to be a mixture of complexes C and **D**.

Similar optical and ESR spectra of complexes **C** and **D** were also observed by using $NaOCH_3$ instead of TMAOH (Tables 1 and 2). Furthermore, the observed optical and ESR parameters of complexes **C** and **D** agreed well with each other (Tables 1 and 2). However, the formation of complexes **C** and **D** was never detected when Fe(III)TPPCl, skatole and TMAOH were mixed at 25 °C by the same mixing molar ratio. This suggests that complexes C and **D** have a short lifetime at 25 °C in our reaction conditions.

When the frozen mixture containing complexes **C** and **D** was annealed at 25 °C for about 5 min, the color of the solution rapidly changed to deep green. The observed absorption spectrum (Fig. 6(c)) gave the absorption maxima at 417, 586 and 625 nm, which agrees with that recorded under nitrogen atmosphere, as mentioned above (Fig. 3(b)). On the other hand, ESR signals due to complexes **C** and **D** completely disappeared, and that of complex **A** was again observed, as shown in Fig. 6(c). Of interest is the fact that a new ESR signal characterized by a large g anisotropy (denoted as complex E; $g_1 = 2.66$, $g_2 = 2.23$, $g_3 = 1.82$) was observed for the annealed solution. Complex **E** would be one of the Fe(III)TPP complexes having a product molecule derived from skatole at the axial position. In fact, GLC measurements demonstrated that about 4% skatole was converted to FA in this reaction mixture. At present, the accurate coordination structure of complex **E** is still equivocal. However, complex **E** was assumed to be a six-coordinate Fe(III)TPP complex, having oxygenous and nitrogenous ligands at the axial positions, because the observed g parameters of complex **E** showed coincidence with those relevant ferric low-spin complexes reported previously, as summarized in Table 1. These observed results suggest that both complexes **C** and **D** were very unstable at 25 °C and were rapidly decomposed within about 5 min at 25 °C. Therefore, complexes **C** and **D** were concluded to be one of the intermediate species formed in the dioxygenation processes of skatole.

ESR Measurements Carried out for Complexes C and D Prepared under $^{17}O_2$ Atmosphere

The pre-degassed reaction mixture composed of Fe(III)TPPCl (1.0 mM, 0.2 ml), skatole (0.4 M, 0.2 ml) and a methanol solution of TMAOH (0.01 M, 0.2 ml) was exposed to 49% enriched $^{17}O_2$ ($I = 5/2$) at −78 °C for about 3 min, by the same method described above. The observed ESR spectrum revealed the formation of complexes **C** and **D**, as shown in Fig. 7(b). The observed g parameters agreed well with those of complexes **C** and **D** prepared under $^{16}O_2$ atmosphere (Fig. 7(a)) (Table 1). The ESR linewidth of the g_3 component (higher field) of complexes **C** and **D** increased by about two times compared to that recorded under $^{16}O_2$ atmosphere. The observed broad ESR signal could be attributed to the unresolved super-hyperfine splittings due to the ^{17}O atom located at the axial position of Fe(III)TPP. The ^{17}O satellite hyperfine lines (27 gauss) were recognized only in the g_3 component, as shown in Fig. 7(b). The stick diagram indicates that the positions of ^{17}O super-hyperfine splittings overlapped with the g_3 component of complex **C**, assuming equidistance spacing. The detection of such satellite splittings provided the evidence that the oxygenous ligand derived from atmospheric oxygen binds at the axial positions of complexes **C** and **D**. This implies that complexes **C** and **D** possess the oxygenous ligand derived from atmospheric molecular oxygen at the axial position of Fe(III)TPP.

TABLE 1. ESR parameters of the intermediate complexes D and E and related ferric high- and low-spin complexes

Complexes	Base	Peroxide	g_1	g_2	g_3	Reference
Complexes A						
Fe(III)TPP($^-OCH_3$)($HOCH_3$)	TMAOH	none	high-spin	6.0	2.0	[a]
	$NaOCH_3$	none	high-spin	6.0	2.0	[a]
	$NaOCH_3$	none	high-spin	6.0	2.0	10
Complexes B						
Fe(III)TPP($^-OCH_3$)$_2$	TMAOH	none	2.487	2.167	1.915	[a]
	$NaOCH_3$	none	2.497	2.166	1.921	[a]
	$NaOCH_3$	none	2.494	2.165	1.941	10
Complexes C						
Fe(III)TPP($^-OCH_3$)($^-$OO-skatole)	TMAOH	Sk [g] + O_2	2.316	2.169	1.952	[a]
	TMAOH	Sk + $^{17}O_2$	2.318	2.167	1.954	[a]
	$NaOCH_3$	Sk + O_2	2.316	2.170	1.951	[a]
Fe(II)TPP(pyridine)$_2$		Sk + O_2	2.31	2.19	1.93	5
Fe(III)($^-OCH_3$)($^-OOC(CH_3)_3$)	$NaOCH_3$	t-BHPO	2.316	2.157	1.952	8
	TBAOH	t-BHPO	2.316	2.150	1.953	8
Fe(III)–Mb [b]–($^-OOC(CH_3)_3$)	TMAOH	t-BHPO	2.350	2.196	1.936	11
Fe(III)–Hb [c]–($^-OOC(CH_3)_3$)	TMAOH	t-BHPO	2.340	2.188	1.940	11
Complexes D						
Fe(III)TPP($^-$OO-skatole)$_2$	TMAOH	Sk + O_2	2.238	2.160	1.964	[a]
	$NaOCH_3$	Sk + O_2	2.233	2.164	1.965	[a]
Fe(III)TPP($^-OOC(CH_3)_3$)$_2$	$NaOCH_3$	t-BHPO	2.242	2.157	1.964	8
	TBAOH	t-BHPO	2.242	2.150	1.964	8
Complex E						
Fe(III)TPPCl–Products [d]	TMAOH	none	2.66	2.23	1.82	[a]
Fe(III)PPIX(OAr) [e]–Pyridine		none	2.61	2.19	1.84	20
Fe(III)PPIX(OAr)–1MeIm [f]		none	2.56	2.21	1.83	20

[a]Present work. [b]Whale myoglobin. [c]Whale hemoglobin. [d]Oxidative products derived from skatole. [e]PPIXDB, protoporphyrin-dibenzoyl ester, OAr, phenolate anion. [f]1-Methylimidazole. [g]Sk, 3-methylindole (skatole).

TABLE 2. Optical spectra recorded for the TDO model reaction system and optical properties of related iron complexes

Complex	Base	Substrate	Atmosphere	Temperature (K)	Absorption[a]				Reference
Fe(III)TPPCl	none	none	N_2	198	417	510	580	690	[b]
	none	none	N_2	298	416	508	575	695	[b]
Complexes A and B									
Fe(III)TPP($HOCH_3$)($^-OCH_3$) and	TMAOH	none	N_2	198	416	586	623		[b]
Fe(III)TPP($^-OCH_3$)$_2$	$NaOCH_3$	none	N_2	198	416	587	632		[b]
Fe(III)TPP($^-OCH_3$)($HOCH_3$)	$NaOCH_3$	none	air	298	420	580	625		10
Fe(III)TPP($^-OCH_3$)$_2$	$NaOCH_3$	none	air	298	438	550	597	638	10
Complexes C and D [d]									
Fe(III)TPP($^-OCH_3$)($^-$OO-skatole)	TMAOH	Sk [c]	O_2	198	421	550	586		[b]
and ($^-$OO-skatole)$_2$	$NaOCH_3$	Sk	O_2	198	422	548	587		[b]
Fe(III)TPP($^-OCH_3$)(OO-t-BHPO)	$NaOCH_3$	t-BHPO	air	77	420	543	571		8
and -($^-$OO-t-BHPO)$_2$ [d]	TMAOH	t-BHPO	air	77	420	543	573		8
Fe(III)TPP($^-$OH)($^-$OOH)	KOH [e]	HOOH	air	77	420	562	605		13
	TPA [f]	HOOH	air	77	420	562	605		13
Fe(III)Mb [g]($^-$OO-t-BHPO)	TMAOH	t-BHPO	air	77	415	542	574		11
Fe(III)Hb [h]($^-$OO-t-BHPO)	TMAOH	t-BHPO	air	77	412	559	593		11

[a]Experimental error at 298 K is within ±2 nm, at 198 and 77 K is within 5 nm. Experimental error in the Soret-band at 77 K is within 8 nm. [b]Present work. [c]Sk, skatole. [d]Optical parameters of the two types complexes were not distinguished. [e]Aqueous KOH solution. [f]TPA, tri-n-propylamine. [g]Whale myoglobin. [h]Whale hemoglobin.

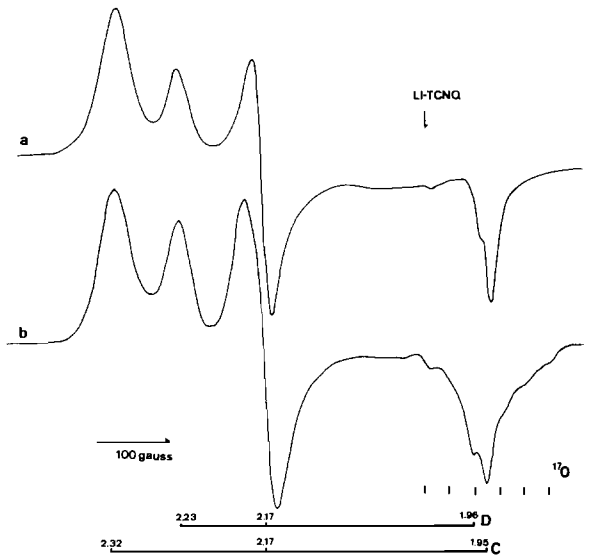

Fig. 7. ESR spectra recorded at 77 K prepared under (a) $^{16}O_2$ and (b) $^{17}O_2$ (49% enriched) atmosphere. The stick diagram indicates the satellite splittings (27 gauss) arising from the ^{17}O atom ($I = 5/2$) binding complex **C**.

Possible Coordination Structure of Complexes C and D

A comparison of the g parameter of complexes **C** and **D** with those of six-coordinate Fe(III)TPP complexes [14, 15] shows that one of the important ESR characters of complexes **C** and **D** is their anomalously small g anisotropy. Recently, the formation of six-coordinate Fe(III)TPP–organic peroxide complexes [8] was demonstrated by means of simultaneous ESR and optical measurements. ESR parameters observed for the six-coordinate Fe(III)TPP($^-OCH_3$)($^-OOC(CH_3)_3$) complex ($g_1 = 2.316, g_2 = 2.157, g_3 = 1.952$) were comparable with those of the present complex **C** ($g_1 = 2.316$, $g_2 = 2.169$, $g_3 = 1.952$). On the other hand, the observed g parameters of complex **D** ($g_1 = 2.238$, $g_2 = 2.160$, $g_3 = 1.964$) showed excellent agreement with those of Fe(III)TPP($^-OOC(CH_3)_3$)$_2$ ($g_1 = 2.242$, $g_2 = 2.157$, $g_3 = 1.964$). By comparison of the g parameters of the Fe(III)TPP–butylperoxide complexes with those observed for complexes **C** and **D**, the present ferric low-spin complexes can be classified into six-coordinate Fe(III)TPP–organic peroxide complexes.

Yoshida *et al.* [5] reported the detection of a low-spin ferric complex ($g_1 = 2.31$, $g_2 = 2.19$, $g_3 = 1.93$) in the model dioxygenase reaction system composed of Fe(II)TPP(pyridine)$_2$ and skatole. The ferric low-spin complex was tentatively explained to be the six-coordinate Fe(III)TPP complex, having the product molecule derived from skatole at the axial position. The observed g parameters were very similar to those of the present complex **C** ($g_1 = 2.316$, $g_2 = 2.169$, $g_3 = 1.952$). From comparison of the g parameter of the Fe(III)TPP–products adduct with complex **C**, the ferric low-spin complex cited in the literature will be identical to complex **C**.

A significant resemblance was also seen in the optical properties of the present complexes **C** and **D**, as compared with the parameters of the Fe(III)TPP–tert-butylperoxide complexes [8]. Complexes **C** and **D** showed characteristic absorption maxima at 421, 550 and 586 nm (Table 2). The Fe(III)TPP–tert-butylperoxide complexes revealed absorption maxima at 420, 543 and 571 nm [7], as summarized in Table 2. In particular, a pair of Q-band absorption maxima was commonly observed for related six-coordinate iron porphyrin–peroxide complexes, such as Fe(III)TPP(^-OH)(^-OOH) [13], and butylperoxide adducts of met-myoglobin and -hemoglobin [11] (Table 2). Accordingly, the optical absorption parameters of complexes **C** and **D** were also rationalized to be those of the six-coordinate iron porphyrin–peroxide complexes.

Taking into consideration the results obtained from $^{17}O_2$ ESR measurements (Fig. 7), we assume that skatole would be converted to a peroxide-type substance by reacting with molecular oxygen in our model system. The hydroperoxide derivative of skatole was regarded to be the most probable candidate for the axial ligand of complexes **C** and **D**. So far, we have never isolated such a hydroperoxide analogue of skatole from the reaction mixture, however, formation of indolenine-3-hydroperoxide derivatives have often been speculated in the auto-oxidation processes of methylated indoles [16]. For example, the hydroperoxide analogues of 2,3-diethyl-indole [17] and tetrahydrocarbazole [18] were actually isolated from their auto-oxidation reactions. Accordingly, the 3-methyl-3-hydroperoxo-indolenine (denoted as HOO-skatole) derivative, is speculated to be the organic peroxide type substance ligating at the axial positions of complexes **C** and **D**. Since organic hydroperoxides, such as tert-butyl-hydroperoxide, prefer the deprotonated form in the presence of alkaline reagents [19], the deprotonated form of HOO-skatole, $^-$OO-skatole, will be the practical axial ligand for complexes **C** and **D**. Therefore, the coordination structure of complex **C** is now assumed to be the six-coordinate Fe(III)TPP($^-OCH_3$)($^-$OO-skatole) complex, which corresponds to the Fe(III)-TPP($^-OCH_3$)($^-$OO-tert-butyl) [8] complex having the skatole peroxide anion instead of the tert-butyl-peroxide anion. In addition, complex **D** is also concluded to be the Fe(III)TPP($^-$OO-skatole)$_2$ complex bearing the $^-$OO-skatole moiety at both the axial positions. Therefore, the coordination structures of complexes **C** and **D** are schematically illustrated in Fig. 8. Complexes **C** and **D** described herein can be formally expressed as the Fe(III)TPP–oxygen–substrate ternary complex, in which the central iron atom and skatole molecule are bridged by two oxygen atoms.

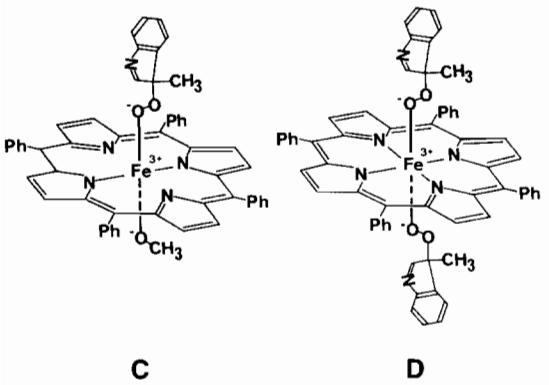

C D

Fig. 8. Probable coordination structures of the six-coordinate complex C, Fe(III)TPP($^-$OCH$_3$)($^-$OO-skatole), and complex D, Fe(III)TPP($^-$OO-skatole)$_2$.

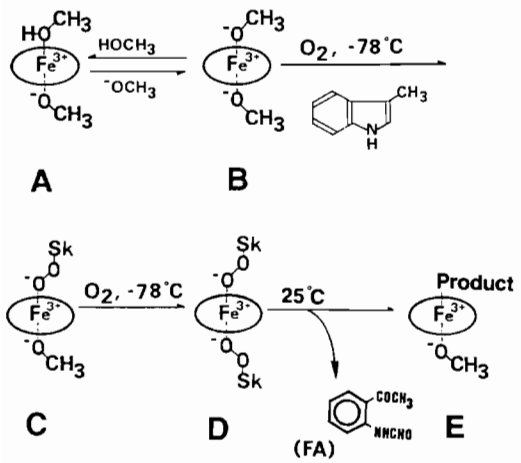

Scheme 3. A possible reaction mechanism of the dioxygenation process of skatole to *o*-formamidoacetophenone occurring in the presence of Fe(III)TPPCl and TMAOH under oxygen atmosphere.

Possible Dioxygenation Mechanism of Skatole

A possible mechanism of the dioxygenation processes of skatole, based on the coordination structures of complexes **C** and **D**, is illustrated in Scheme 3. In the absence of skatole, addition of TMAOH to Fe(III)TPPCl results in the formation of the ferric high-spin complex **A**, Fe(III)TPP(HOCH$_3$)($^-$OCH$_3$), and complex **B**, Fe(III)TPP($^-$OCH$_3$)$_2$. Complexes **A** and **B** were very stable in ambient conditions, and the optical and ESR parameters were scarcely perturbed by anaerobic addition of substrate skatole at –78 °C. When dry oxygen gas was introduced into the reaction mixture at –78 °C, the generation of complexes **C** and **D** began. The ESR signal intensity of complexes **C** and **D** showed concomitant increase when the reaction mixture was kept at –78 °C under oxygen atmosphere, while the ESR signals of complexes **A** and **B** almost disappeared. The successive ESR spectral changes started from complexes **A** and **B** to complexes **C** and **D** are interpreted as an axial ligand exchange reaction occurring between the methoxide anion and the $^-$OO-skatole anion generated in the reaction mixture. This suggests that the concentration of the deprotonated $^-$OO-skatole anion concomitantly increased depending upon the reaction time at –78 °C; the reaction proceeds toward the right hand side when holding the reaction mixture at –78 °C under oxygen atmosphere. At present, the accurate reaction mechanism of $^-$OO-skatole formation is still equivocal, however, complexes **A** and **B** are thought to play an important role in the generation of the $^-$OO-skatole anion by utilizing molecular oxygen because the dioxygenation of skatole was completely inhibited in the absence of both Fe(III)-TPPCl and TMAOH in our reaction system (Fig. 1).

The thaw-and-freezing ESR and optical measurements demonstrated that complexes **C** and **D** were very unstable at 25 °C, and were readily decomposed to complexes **A** and **E** (Fig. 6(c)), having the product molecule at the axial position. In fact, GLC measurements justified the generation of a dioxygenated product (FA) in the reaction mixture annealed at 25 °C for about 5 min, indicating that complexes **C** and **D** will play an important role in converting the axially ligating $^-$OO-Sk molecule to FA. The two oxygen atoms involving in the axially ligating $^-$OO-Sk moiety are thought to be inserted into the indole ring (above 25 °C), after cleavage of the iron–oxygen bond (Scheme 3). Complexes **C** and **D** could correspond to the activated EMSO$_2$* intermediate species (Sceme 1) assumed in the reaction processes of TDO. Several TDO model reaction systems have been elaborated to understand the chemical reactivity of TDO [3–6], however such a metal–oxygen–substrate ternary intermediate complex has scarcely been detected, to our present knowledge. The intermediate complexes **C** and **D** are a practical model complex for the EMSO$_2$* intermediate species frequently assumed in the reaction processes of TDO. Further investigations to understand the mechanism of oxygen activation occurring in the present system are now in progress with the aid of kinetic ESR and optical spectral measurements.

Acknowledgements

The authors express sincere thanks to Professor Dr Hiromu Sakurai of Tokushima University for helpful scientific discussion about heme chemistry. We also express our deep gratitude to Miss Tamie Ishida of the Advanced Instrumental Center for Chemical Analysis, Ehime University, for her kind help with GC-MS measurements. This work was partially supported by a Grant-in-Aid for Scientific Research from the Ministry of Education, Science and Culture, Japan.

References

1 O. Hayaishi, S. Rothberg, A. H. Mehler and Y. Saito, *J. Biol. Chem., 229* (1957) 889; W. N. Poillon, H. Maeno, M. Koike and P. Feigelson, *J. Biol. Chem., 244* (1969) 3447; G. Schutz and P. Feigelson, *J. Biol. Chem., 247* (1972) 5327; O. Hayaishi, in T. E. King, H. Mason and M. Morrison (eds.), *Oxidases and Related Redox Systems,* Pergamon, New York, 1982, p. 787.

2 Y. Ishimura, M. Nozaki, O. Hayaishi, T. Nakamura, M. Tamura and I. Yamazaki, *J. Biol. Chem., 245* (1970) 3593.

3 A. Nishinaga, *Chem. Lett.,* (1975) 273.

4 K. Uchida, M. Soma, S. Naito, T. Onishi and K. Tamaru, *Chem. Lett.,* (1978) 471.

5 Z. Yoshida, H. Sugimoto and H. Ogoshi, in D. Dolphin, C. McKenna, Y. Murakami and I. Tabushi (eds.), *Biomimetic Chemistry,* Advances in Chemistry Series No. 191, American Chemical Society, 1980, p. 307.

6 M. N. Dufour-Ricroch and A. Gaudemer, *Tetrahedron Lett.,* (1976) 4079.

7 K. Tajima, K. Ishizu, H. Sakurai and H. Ohya-Nishiguchi, *Biochem. Biophys. Res. Commun., 135* (1986) 972.

8 K. Tajima, J. Jinno, K. Ishizu, H. Sakurai and H. Ohya-Nishiguchi, *Inorg. Chem., 28* (1989) 709.

9 A. D. Adler, F. R. Longo and V. Vardi, *Inorg. Synth., 16* (1976) 213.

10 T. Ohtsuka, T. Ohya and M. Sato, *Inorg. Chem., 24* (1985) 776.

11 K. Tajima, *Inorg. Chim. Acta, 169* (1990) 211.

12 J. D. Lipscomb, J. B. Howard and J. M. Wood, in T. E. King, H. Mason and M. Morrison (eds.), *Oxidases and Related Redox Systems,* Pergamon, New York, 1982, p. 483.

13 K. Tajima, *Inorg. Chim. Acta, 163* (1989) 115; K. Tajima, M. Shigematsu, J. Jinno, K. Ishizu and H. Ohya-Nishiguchi, *J. Chem. Soc., Chem. Commun.,* (1990) 144; K. Tajima, M. Shigematsu, J. Jinno, Y. Kawano, K. Mikami, K. Ishizu and H. Ohya-Nishiguchi, *Biochem. Biophys. Res. Commun., 166* (1990) 924.

14 F. A. Walker, D. Reis and V. Balk, *J. Am. Chem. Soc., 106* (1984) 6888.

15 H. Sakurai and T. Yoshimura, *J. Bioinorg. Chem., 24* (1985) 75.

16 P. Brown and R. C. Cookson, *Tetrahedron, 24* (1968) 2551.

17 E. Leete, *J. Am. Chem. Soc., 83* (1961) 3645.

18 R. J. S. Beer, T. Broadhurst and A. Robertson, *J. Chem. Soc.,* (1952) 4946.

19 A. J. Evertt and G. J. Minkoff, *Trans. Faraday Soc., 44* (1953) 745; D. Swein (ed.), *Organic Peroxides,* Vols. 1 and 2, Wiley-Interscience, New York, 1971.

20 R. Quinn, M. Nappa and J. S.-Valentine, *J. Am. Chem. Soc., 104* (1982) 2588.